Engineering topological state transfer in four-period Su–Schrieffer–Heeger chain

Xi-Xi Bao(包茜茜)[1], Gang-Feng Guo(郭刚峰)[1], and Lei Tan(谭磊)[1,2,†]

[1] *Lanzhou Center for Theoretical Physics, Key Laboratory of Theoretical Physics of Gansu Province, Lanzhou University, Lanzhou* 730000, *China*
[2] *Key Laboratory for Magnetism and Magnetic Materials of the Ministry of Education, Lanzhou University, Lanzhou* 730000, *China*

(Received 20 April 2022; revised manuscript received 10 June 2022; accepted manuscript online 27 June 2022)

An extended Su–Schrieffer–Heeger (SSH) model containing four periods of the hopping coefficients, called SSH4 model, is constructed to explore robust quantum state transfer. The gap state protected by the energy gap plays the role of the topological channel where the particle initially located at the last lattice site has the probability to arise at the first and all even lattice sites equally. Serving those sites as ports, a multi-port router can be realized naturally, and the fidelity reaches unity in a wide range of parameters under the long chain and random disorder. Further, when we reduce the third intracell hopping to a small value, the occupancy probability of the second lattice site in every unit cell will reduce to zero, by which a new topological router can be induced. In addition, our SSH4 model can work as a $1/3$ beam splitter. Namely, the particle initially occupies the first lattice site and finally appears with equal probability at three lattice sites. We can also realize a $1/2$ beam splitter. Our four-period SSH model provides a novel way for topological quantum information processing and can engineer two kinds of quantum optical devices.

Keywords: topological state transfer, robust, high fidelity

PACS: 03.65.Vf, 03.67.–a, 05.60.Gg **DOI:** 10.1088/1674-1056/ac7bfe

1. Introduction

Large-scale quantum information processing has drawn a great deal of attention in recent years.[1–16] Undoubtedly, the core concept to achieve quantum information transmission between distant nodes is the robust quantum state transfer.[17–21] Various systems have been explored to realize this process, for example, cavity electromechanical systems,[22–24] spin chain and spin-wave engineering,[5,6,18,21,25] and quantum dots.[26,27] However, one can find that the imperfect (disorder, defect and impurities) of the usual devices and the environment noise inevitably have a negative influence on the fidelity of quantum state transfer.

The role of topology in the field of physics has been studied in many fashions.[28–33] To date, we know that the typical feature of the topological insulators is the existence of the robust edge state protected by the energy gap,[34–38] which provides global protection with respect to the local deformations of the system.[39–43] The invariance under continuous deformations endows the topological insulators with boundless potential applications in quantum information processing and engineering. Correspondingly, there has been a significant surge of interest in investigating robust quantum state transfer using the topological system.[9,12,15,28,44–47] In Ref. [28], Dlaska *et al.* displayed the robust quantum state transfer via topologically protected edge pumping in a two-dimensional topological spin system. Mei *et al.*[44] showed robust quantum state transfer via topological edge states in superconducting qubit chain. Zheng *et al.*[46] proposed an effective scheme to realize robust quantum state transfer with the topological protected channel in a superconducting flux qubit chain with controlling by defect. In addition, Qi *et al.*[47] studied the one-dimensional modulated Su–Schrieffer–Heeger chain and implemented the various kinds of topological routers. However, the realization of the topological channel with multiple functions in practical applications is still an open question. Regretfully, most of the previous studies only involve a single quantum state transition.

Motivated by the discussions mentioned above, we construct a topological channel in an extended SSH model with four-period hopping coefficients in one unit cell, dubbed SSH4, to study the robust quantum state transfer. In our multi-band system, the topological channel is determined by the gap state protected by the energy gap, in which the particle initially accommodated at the last lattice site will arise in the first and all even lattice sites equally. Then, a multi-port router, being immune to mild-disorder, can be realized if we treat those sites as ports. Further, the probability of the second lattice sites in every unit cell will reduce to zero in certain cases, which demonstrates that a new topological router can be obtained. In addition, our SSH4 model can have the application of $1/3$ beam splitter. Namely, the particle occupied at the first lattice site will appear with equal probability at three lattice sites with time evolution. This system can realize a $1/2$ beam splitter. Our four-period SSH model can engineer two kinds of quantum optical devices, which is of great significance for quantum information processing.

This paper is organized as follows. In Section 2 we present the extended SSH4 chain with four-period hopping coefficients in one unit cell. In Section 3 it is demonstrated that

†Corresponding author. E-mail: tanlei@lzu.edu.cn

© 2023 Chinese Physical Society and IOP Publishing Ltd

our multi-band system can realize different types of topological routers with multiple output ports and we explore the effect of the third intracell hopping strength on topological router. In Section 4 we display that our model can realize a $1/3$ and $1/2$ topological beam splitter. Finally, the conclusions are presented in Section 5.

2. The four-period SSH chain

We consider a one-dimensional four-period SSH chain comprised of $4N+1$ lattice sites, with N even, as schematically shown in Fig. 1. In this chain, each unit cell contains four lattice sites labeled by A, B, C, and D, respectively. The extended SSH chain can be described by

$$H = \sum_n t_1 C^\dagger_{n,A} C_{n,B} + t_2 C^\dagger_{n,B} C_{n,C} + t_3 C^\dagger_{n,C} C_{n,D} + t_4 C^\dagger_{n,D} C_{n+1,A} + J_n C^\dagger_{1,A} C_{n+1,A} + \text{H.c.}, \quad (1)$$

where $C^\dagger_{n,Q}$ $(Q = A,B,C,D)$ and $C_{n,Q}$ are the creation and annihilation operators on sublattices A, B, C, D of the nth unit cell; t_1, t_2 and t_3 are the intracell hopping amplitudes; t_4 is the intercell hopping amplitude. The long-range hopping strengths are represented by J_n in which the first site A_1 can jump to an arbitrary A-type site in the nth unit cell. For the sake of simplicity, we choose the long-range hopping amplitudes $J_1 = J_2 = \cdots = J_N \equiv J$ in this study.

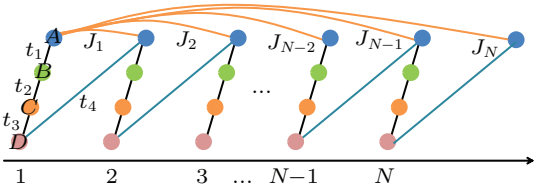


Fig. 1. Schematic diagram of the one-dimension extended SSH chain with odd number $L = 4N+1$. Here, N is the number of unit cell and each one contains four lattice sites labeled by A_n, B_n, C_n, and D_n $(n = 1,2,\ldots,N)$. The intracell hoppings are t_1, t_2, and t_3, respectively. The intercell hopping is t_4, and the long-range hopping is J_n.

3. Different types of topological router in four-period SSH chain

In this section, we take the parameter $t_1 = 1+\cos\theta$, $t_2 = 2$, and $t_4 = J = 1-\cos\theta$. Next, the quantum state transfer will be explored by selecting different values of t_3.

3.1. Topological router induced by $t_3 = t_2$

In this subsection, we focus on a strong intracell hopping $t_3 = t_2 = 2$. The corresponding energy spectrum, as shown in Fig. 2(a), always has a state in the energy gap, which provides a cornerstone to realize the robust quantum state transfer. Further, the distribution of the gap states with the varying of θ is displayed in Fig. 2(b). It can be found that the gap state is occupied at the last site when $\theta = 0$, whereas it is equally localized at $A_1, B_1, D_1, \ldots, D_N$ with $\theta = \pi$. The numerical results mentioned above can be understood physically as follows. When $\theta = 0$, the strengths of all intracell hopping amplitudes are larger than those of the intercell hopping and long-range hooping amplitudes, i.e., $t_1, t_2, t_3 = 2 > t_4 = J = 0$. This phenomenon is similar to fully dimerized limits.[48] Namely, these four sublattices in each unit cell form a tetramer, which causes the final lattice site being isolated. Therefore, the gap state occupies the last site totally. Further, when $\theta = \pi$, corresponding to $t_1 = 0$ and $t_2 = t_3 = t_4 = J = 2$, the four-band SSH chain can be divided into several components in the unit of three sites. According to Refs. [47,48], we find that our system contains two kinds of domain walls, which are expressed as two trimers. A set is C_n, B_n, and D_n, and the other set is A_n $(n \neq 1)$, A_1, and D_n. As a result, the gap state is mainly localized at sites A_1, B_1, $D_1, \ldots$, and D_N with $\theta = \pi$. This transfer process by changing the parameter θ indicates that the gap state can be served as the topological channel to realize the state transfer between the initial state $|\Psi\rangle_\text{i} = |0,0,0,\ldots,0,1\rangle$ and the final state $|\Psi\rangle_\text{f} = \frac{1}{\sqrt{2N+1}}|1,1,0,1,\ldots,1,0\rangle$.

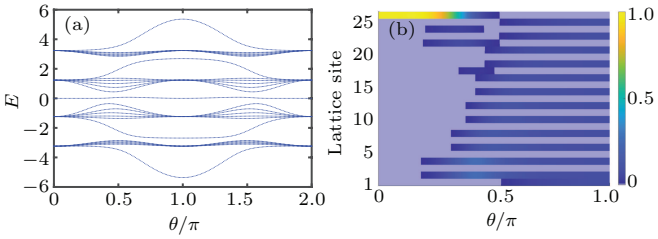


Fig. 2. (a) The energy spectra of the generalized SSH chain with $t_1 = 1+\cos\theta$, $J = t_4 = 1-\cos\theta$ and $t_2 = t_3 = 2$. It always has a gap state. (b) The corresponding state distribution of gap state. When $\theta = 0$, the gap state gathers toward the last lattice site but $\theta = \pi$, the gap state localizes at the site of A_1, B_1, $D_1, \ldots$, and D_N.

To further estimate this result, we take the parameter θ as

$$\theta(t) = \Omega t, \quad (2)$$

where Ω represents the ramping frequency, and t is the time.[44] Then, we can perform the time evolution of the initial state by the Schrödinger equation $\mathrm{i}\frac{\partial}{\partial t}|\Psi\rangle_t = H(\theta_t)|\Psi\rangle_t$ (here, we set $\hbar = 1$ for simplicity). As we all know, the quantum state transfer by dint of the gap state is protected by the energy gap. In Fig. 3(a), the energy gap ΔE (the gap state and the nearest state of the up band) versus the number of the lattice sites is plotted. Obviously, as the number of unit cells increases, the energy gap becomes smaller. Meanwhile, the adiabatic conditions need to be obeyed in the process of state evolution. Therefore, if the size of the system is larger, Ω will be smaller. On the contrary, a small size means that there is a larger Ω, and the adiabatic condition is easier to achieve.[46] In addition, Fig. 3(b) indicates that the fidelity between the ideal state and the final state keeps a wide plateau at the value of unity when $L = 25$, which ensures perfectly the quantum state transfer in a long chain. Moreover, in order to verify this

result, in Fig. 4(a), when $\Omega = 0.0038$, the numerical results unveil that the state transfer between $|\Psi\rangle_{\rm i} = |0,0,0,\ldots,0,1\rangle$ and $|\Psi\rangle_{\rm f} = \frac{1}{\sqrt{2N+1}}|1,1,0,1,\ldots,1,0\rangle$ can be achieved.

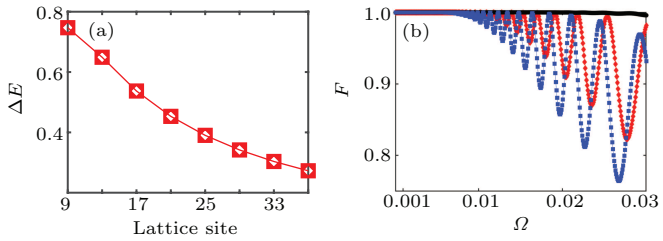


Fig. 3. (a) The energy gap (the gap state and the up band) ΔE versus the size of the lattice site. (b) The fidelity of the topological router versus the ramping speed Ω. The black circle, red triangle and blue square lines correspond to the size of the lattice as $L = 9$, $L = 25$, and $L = 29$, respectively. Other parameters are $t_1 = 1 + \cos\theta$, $J = t_4 = 1 - \cos\theta$, and $t_2 = t_3 = 2$.

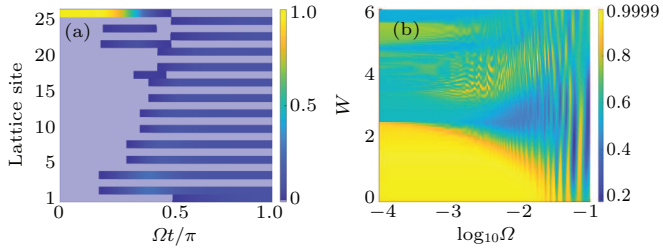


Fig. 4. (a) The state transfer process of $|0,0,0,\ldots,0,1\rangle$ corresponding to $\Omega = 0.0038$. (b) The fidelity between the evolved final state and the ideal final state versus the ramping speed Ω and disorder W. Here, $t_1 = 1 + \cos\theta$, $J = t_4 = 1 - \cos\theta$, and $t_2 = t_3 = 2$.

Finally, we note that there always exists imperfection in the real system, such as defects and impurities. The Hamiltonian with imperfection, i.e., on-site disorder, has the form of

$$\begin{aligned} H =& \sum_n W\delta(C^\dagger{}_{n,A}C_{n,A} + C^\dagger_{n,B}C_{n,B} \\ &+ C^\dagger_{n,C}C_{n,C} + C^\dagger_{n,D}C_{n,D}) \\ &+ \sum_n t_1 C^\dagger{}_{n,A}C_{n,B} + t_2 C^\dagger{}_{n,B}C_{n,C} + t_3 C^\dagger{}_{n,C}C_{n,D} \\ &+ t_4 C^\dagger{}_{n,D}C_{n+1,A} + J_n C^\dagger{}_{1,A}C_{n+1,A} + \text{H.c.}, \end{aligned} \tag{3}$$

where W is the strength of the disorder, and δ is a random number in the range of $[-0.5, 0.5]$ uniformly. In this case, the fidelity between the evolved state and the ideal final state versus the ramping speed Ω and the disorder strength W is numerically displayed in Fig. 4(b). The yellow regions undoubtedly show that, for the slow enough ramping speed $\log_{10}(\Omega) < -2.5$ and the disorder strength $W < 2.5$, the state transfer between $|\Psi\rangle_{\rm i}$ and $|\Psi\rangle_{\rm f}$ can be realized with high fidelity.

3.2. A topological router by $t_3 = 0.015$

We have demonstrated that a multi-port topology router can be formed if $t_3 = t_2 = 2$. In this subsection, we take the parameter $t_3 = 0.015$ to explore the quantum state transfer.

As we will exhibit, the topological channel can be changed essentially when we reduce the parameter t_3 to 0.015, which implies that it can achieve another type of router. In this way, we reveal the energy spectrum in Fig. 5(a), in which the gap state as a topological channel still exists while the minimum energy gap is small, as shown in Fig. 5(b). Further, the distribution of the gap states is shown in Fig. 5(c). Obviously, the new gap state is localized at the last site primitively, while finally localized at A_1, D_1, $D_2,\ldots,D_N$ uniformly, which indicates that the feasibility of implementing the state transfer between the initial state $|\Psi\rangle_{\rm i} = |0,0,0,\ldots,0,1\rangle$ and the final state $|\Psi\rangle_{\rm f} = \frac{1}{\sqrt{N+1}}|1,0,0,1,0,0,0,1,\ldots,0,0,0,1,0\rangle$.

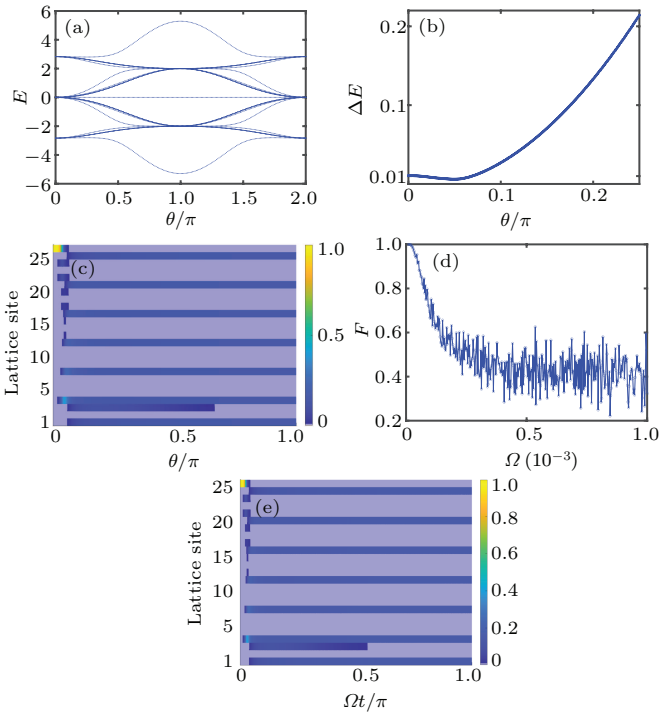


Fig. 5. (a) The energy spectra of the generalized SSH chain with $t_1 = 1 + \cos\theta$, $J = t_4 = 1 - \cos\theta$ and $t_2 = 2$ and $t_3 = 0.015$. (b) The distribution of gap state. (c) The fidelity of the state transfer between the evolved final state and the ideal final state versus the varying rate of θ. (d) The state transfer process corresponding to $\Omega = 10^{-5}$.

To further confirm this result, we plot the fidelity of the state transfer versus the ramping speed Ω, as shown in Fig. 5(d). A small Ω is required to meet the adiabatic evolution condition since the energy gap is narrow at this point. Moreover, to make the results more intuitive, in Fig. 5(e), we choose an appropriate value of $\Omega = 10^{-5}$. This numerical result reveals exactly the state transfer between $|\Psi\rangle_{\rm i}$ and $|\Psi\rangle_{\rm f}$. Compared with Fig. 4(a), we find that when t_3 reduces to a small value, the probability of the second lattice site in every unit cell will reduce to zero, by which a new topological router can be induced.

The processes mentioned above can be comprehended as follows. When $\theta = 0$, all intracell hopping amplitudes are large than intercell hopping and long-range hooping amplitudes, namely, $t_1, t_2, t_3 > t_4 = J$, which leads to the four sublat-

tice sites belonging to one unit cell and the final lattice being isolated. Hence, all states locates at the last site. On the other hand, when $\theta=\pi$, A_n, A_1, and D_n constitute a domain wall.[48] Therefore, the sites A_1 and D_n can be isolated. Finally, the gap state is localized at sites A_1, $D_1,\ldots$, and D_n uniformly.

From above all, two types of topological routers can be realized in our SSH4 model, only via designing the third intracell hopping t_3 appropriately. Therefore, we can control this parameter to realize the distribution of information to some ports.

4. The topological beam splitter

We have discussed the impact of t_3 on the topological channel. Here, we propose the question for our long SSH4 chain: if other parameters are changed, is there a new channel for state transfer precisely? In the following, the parameters t_1 and t_4 change as $t_1=J=1-\cos\theta$ and $t_4=1+\cos\theta$, respectively. We find that, in this set of parameters, our SSH4 system can functionally implement the $1/3$ and $1/2$ topological beam splitter similar to traditional beam splitter[49–52] in quantum optics.

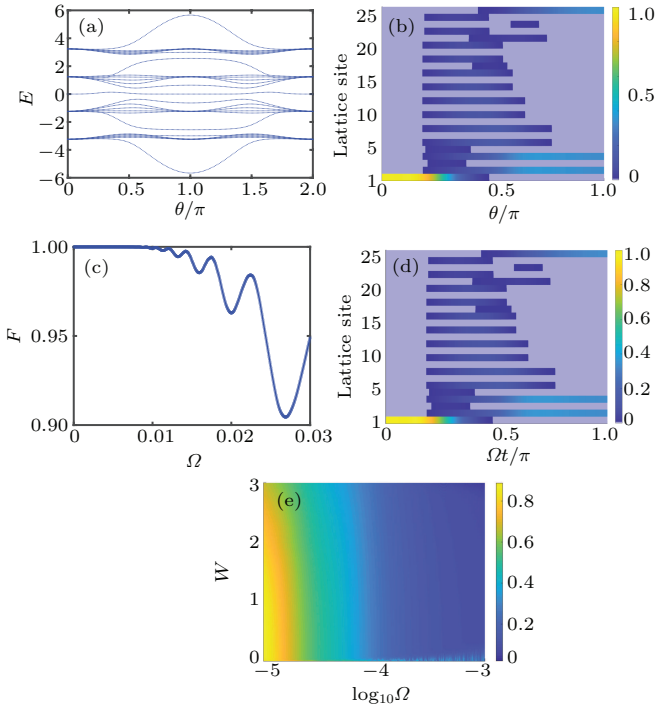


Fig. 6. (a) The energy spectra of the extended SSH chain with $t_4=1+\cos\theta$, $J=t_1=1-\cos\theta$, $t_2=t_3=2$. (b) The corresponding the distribution of gap state. (c) The fidelity of the state transfer between $|1,0,0,\ldots,0,0\rangle$ and $|0,1/3,0,1/3,0,0,\ldots,0,0,1/3\rangle$ versus the varying rate of θ. (d) The state transfer process corresponding to $\Omega=0.006$. (e) The fidelity between the evolved final state and the ideal final state versus the ramping speed Ω and disorder W.

4.1. The $1/3$ topological beam splitter

Under this condition, we further choose $t_2=t_3=2$ to investigate the state transfer. As shown in Fig. 6(a), the energy spectrum tells us that the gap state always exists in our long SSH4 chain. The corresponding distribution of the gap state is shown in Fig. 6(b). It can be found that the gap state is mainly localized at the first site in $\theta=0$, and yet it will pile up at the second, the fourth and the last sites with the same probability in $\theta=\pi$ eventually. One can then get some information that, through the gap state, the state transfer between the state $|1,0,0,\ldots,0\rangle$ and $|0,1/3,0,1/3,0,\ldots,0,0,1/3\rangle$ can be achieved. To estimate the above result more precisely, one can take $\theta=\Omega t$ and utilize the time-dependent Hamiltonian to evolve the initial state $|1,0,0,\ldots,0\rangle$. In Fig. 6(c), the fidelity between the ideal state $|0,1/3,0,1/3,0,\ldots,0,0,1/3\rangle$ and the evolved final state versus the parameter Ω is displayed. The numerical results clarify that some value of Ω can ensure the achievement of the state transfer between the initial state and evolved state. A concrete example can be revealed in Fig. 6(d) with $\Omega=0.006$, and we find that the state initially in the first site can be transferred to the second, the fourth and the last site with the same distributions.

As we explained above, the process of the realization of the topological router is immune to on-site disorder. Here, we also numerically show that the effect of the on-site disorder on our beam splitter. The disorder has the form of $\sum_n W\delta(C^\dagger_{n,A}C_{n,A}+C^\dagger_{n,B}C_{n,B}+C^\dagger_{n,C}C_{n,C}+C^\dagger_{n,D}C_{n,D})$ (with W being the disorder strength and δ being the a random number within $[-0.5, 0.5]$). In Fig. 6(e), the fidelity between the evolved state and the ideal final state is displayed versus the ramping speed Ω and the disorder strength W. It can be found that the state transfer between $|\Psi\rangle_{\rm i}$ and $|\Psi\rangle_{\rm f}$ can be realized with high fidelity under slow enough ramping speed and mild disorder.

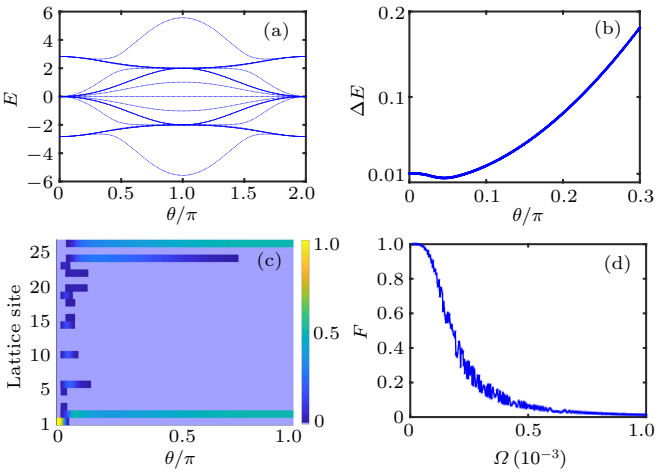


Fig. 7. (a) The energy spectra of the generalized SSH chain with $t_1=1+\cos\theta$, $J=t_4=1-\cos\theta$, $t_2=0.015$, and $t_3=2$. (b) The energy gap at $\theta\in[0,0.3\pi]$. (c) The distribution of gap state. (d) The fidelity of the state transfer between the evolved final state and the ideal final state versus the ramping speed Ω.

4.2. The $1/2$ topological beam splitter

Analogously, one can choose $t_2=0.015$ and $t_3=2$. In Figs. 7(a) and 7(b), there always possess the energy gap even though t_2 is small, which can be used as a topological channel to achieve topological state transfer. As shown in Fig. 7(c), we

plot the distribution of the state with θ. It can be found that the initial state ($\theta = 0$) lies in the first sites while the final states ($\theta = \pi$) occupy the second and the last sites, which illustrates that the gap state can be served as a channel to actualize a $1/2$ beam splitter.[49] Further, to prove our idea, one can choose $\theta = \Omega t$ and numerically calculate the fidelity in Fig. 7(d). It can be found that the fidelity $F = 1$ when Ω is small, implying that our SSH4 system can functionally implement the $1/2$ topological beam splitter.

5. Conclusion

We have constructed an SSH4 model containing four periods of the hopping coefficients to investigate robust quantum state transfer. A topologically protected channel where the particle initially pinned at the last lattice site and finally appeared equally at multiple lattice sites can be formed. Then, a multi-port router can be realized provided that we treat those sites as ports. Moreover, the transfer fidelity displays a wide plateau at the value of unity even if the disorders are considered. When the third intracell hopping reduces to a small value, it can generate a new topological router in which the occupancy probability of all the second lattice sites becomes zero. In addition, the long SSH4 chain can have the function of a $1/3$ beam splitter. Namely, the particle initially occupies the first lattice site and finally appears with equal probability at three lattice sites. We can also realize a $1/2$ beam splitter. The SSH4 system may play a key role in multiple function topological channel, which is vital in quantum information processing. Our four-period SSH model can engineer two kinds of quantum optical devices, which provides the potential applications for topological quantum information processing.

Acknowledgements

Project supported by the National Natural Science Foundation of China (Grant Nos. 11874190, 61835013, and 12047501), and the Supercomputing Center of Lanzhou University.

References

[1] Saffman M, Walker T G and Mølmer K 2010 *Rev. Mod. Phys.* **82** 2313
[2] Duan L M and Monroe C 2010 *Rev. Mod. Phys.* **82** 1209
[3] Suter D and Álvarez G A 2016 *Rev. Mod. Phys.* **88** 041001
[4] Kay A 2009 *Phys. Rev. A* **79** 042330
[5] Paganelli S, Lorenzo S, Apollaro T J G, Plastina F and Giorgi G L 2013 *Phys. Rev. A* **87** 062309
[6] Lorenzo S, Apollaro T J G, Paganelli S, Palma G M and Plastina F 2015 *Phys. Rev. A* **91** 042321
[7] Plenio M B, Hartley J and Eisert J 2004 *New J. Phys.* **6** 36
[8] Silveri M P, Kumar K S, Tuorila J, Li J, Vepsäläinen A, Thuneberg E V and Paraoanu G S 2015 *New J. Phys.* **17** 043058
[9] Vijay S and Fu L 2016 *Phys. Rev. B* **94** 235446
[10] Stannigel K, Rabl P, Sørensen A S, Lukin M D and Zoller P 2011 *Phys. Rev. A* **84** 042341
[11] Chen Q and Feng M 2010 *Phys. Rev. A* **82** 052329
[12] Zhang Z T and Yu Y 2013 *Phys. Rev. A* **87** 032327
[13] Li D X and Shao X Q 2018 *Phys. Rev. A* **98** 062338
[14] Stannigel K, Komar P, Habraken S J M, Bennett S D, Lukin M D, Zoller P and Rabl P 2012 *Phys. Rev. Lett.* **109** 013603
[15] Rips S and Hartmann M J 2013 *Phys. Rev. Lett.* **110** 120503
[16] Chen J, Nurdin H I and Yamamoto N 2020 *Phys. Rev. Appl.* **14** 024065
[17] Cirac J I, Zoller P, Kimble H J and Mabuchi H 1997 *Phys. Rev. Lett.* **78** 3221
[18] Christandl M, Datta N, Ekert A and Landahl A J 2004 *Phys. Rev. Lett.* **92** 87902
[19] Wang Y D and Clerk A A 2012 *Phys. Rev. Lett.* **108** 153603
[20] Zhang J, Peng K and Braunstein S L 2003 *Phys. Rev. A* **68** 013808
[21] Yao N Y, Jiang L, Gorshkov A V, Gong Z X, Zhai A, Duan L M and Lukin M D 2011 *Phys. Rev. Lett.* **106** 040505
[22] Zheng S B and Guo G C 2000 *Phys. Rev. Lett.* **85** 2392
[23] Yang C P, Chu S I and Han S 2003 *Phys. Rev. A* **67** 042311
[24] Yang C P, Chu S I and Han S 2004 *Phys. Rev. Lett.* **92** 117902
[25] Bose S 2003 *Phys. Rev. Lett.* **91** 207901
[26] Brandes T and Vorrath T 2002 *Phys. Rev. B* **66** 075341
[27] He Y, He Y M, Wei Y J, Jiang X, Chen K, Lu C Y, Pan J W, Schneider C, Kamp M and Höfling S 2017 *Phys. Rev. Lett.* **119** 060501
[28] Dlaska C, Vermersch B and Zoller P 2017 *Quantum Sci. Technol.* **2** 015001
[29] Li L, Xu Z and Chen S 2014 *Phys. Rev. B* **89** 085111
[30] Gröning O, Wang S, Yao X, Pignedoli C A, Borin Barin G, Daniels C, Cupo A, Meunier V, Feng X, Narita A, Müllen K, Ruffieux P and Fasel R 2018 *Nature* **560** 209
[31] Di Liberto M, Recati A, Carusotto I and Menotti C 2016 *Phys. Rev. A* **94** 062704
[32] Bao X X, Guo G F, Du X P, Gu H Q and Tan L 2021 *J. Phys.: Condens. Matter* **33** 185401
[33] Guo G F, Bao X X and Tan L 2021 *New J. Phys.* **23** 123007
[34] Hasan M Z and Kane C L 2010 *Rev. Mod. Phys.* **82** 3045
[35] Qi X L and Zhang S C 2011 *Rev. Mod. Phys.* **83** 1057
[36] Chiu C K, Teo J C Y, Schnyder A P and Ryu S 2016 *Rev. Mod. Phys.* **88** 035005
[37] Bansil A, Lin H and Das T 2016 *Rev. Mod. Phys.* **88** 021004
[38] Shen S Q 2012 *Topological Insulators Dirac Equation in Condensed Matters.* In *Springer Series in Solid-State Sciences* vol. 174 (Berlin: Springer)
[39] Wu Q, Du L and Sacksteder V E 2013 *Phys. Rev. B* **88** 045429
[40] Chen L, Wang Z F and Liu F 2013 *Phys. Rev. B* **87** 235420
[41] Paananen T and Dahm T 2013 *Phys. Rev. B* **87** 195447
[42] Malki M and Uhrig G S 2017 *Phys. Rev. B* **95** 235118
[43] Brouwer P W, Duckheim M, Romito A and von Oppen F 2011 *Phys. Rev. B* **84** 144526
[44] Mei F, Chen G, Tian L, Zhu S L and Jia S 2018 *Phys. Rev. A* **98** 012331
[45] Qi L, Wang G L, Liu S, Zhang S and Wang H F 2020 *Phys. Rev. A* **102** 022404
[46] Zheng L N, Qi L, Cheng L Y, Wang H F and Zhang S 2020 *Phys. Rev. A* **102** 012606
[47] Qi L, Yan Y, Xing Y, Zhao X D, Liu S, Cui W X, Han X, Zhang S and Wang H F 2021 *Phys. Rev. Research* **3** 023037
[48] Asbóth J, Oroszlány L and Pályi A 2016 *A Short Course on Topological Insulators.* In *Lecture Notes in Physics* vol. 919 (Berlin: Springer)
[49] Qi L, Wang G L, Liu S, Zhang S and Wang H F 2020 *Phys. Rev. A* **102** 022404
[50] Schonbrun E, Wu Q, Park W, Yamashita T and Summers C J 2006 *Opt. Lett.* **31** 3104
[51] Cassettari D, Hessmo B, Folman R, Maier T and Schmiedmayer J 2000 *Phys. Rev. Lett.* **85** 5483
[52] Chen C C, Chien H D and Luan P G 2004 *Appl. Opt.* **43** 6187